Title
Strange-Particle Production by 1170-MeV/c pi- Mesons

Permalink

Author
Anderson, Jared Arnold

Publication Date
1963-05-27

University of California

Ernest O. Lawrence Radiation Laboratory

STRANGE-PARTICLE PRODUCTION BY 1170-MeV/c π^- MESONS

Berkeley, California

UNIVERSITY OF CALIFORNIA

Lawrence Radiation Laboratory
Berkeley, California

Contract No. W-7405-eng-48

STRANGE-PARTICLE PRODUCTION BY 1170-MeV/c π^- MESONS IN HYDROGEN

Jared Arnold Anderson

(Ph. D. Thesis)

May 27, 1963

STRANGE-PARTICLE PRODUCTION BY 1170-MeV/c π-MESONS IN HYDROGEN

Contents

STRANGE-PARTICLE PRODUCTION BY 1170-MeV/c π-MESONS IN HYDROGEN

Jared Arnold Anderson

Lawrence Radiation Laboratory
University of California
Berkeley, California

May 27, 1963

ABSTRACT

Production of $\Lambda + K^0$, $\Sigma^0 + K^0$, and $\Sigma^- + K^+$ by 1170-MeV/c π^- mesons has been studied in the Lawrence Radiation Laboratory 72-inch hydrogen bubble chamber. Cross sections, angular distributions, and polarizations are presented. The polarization of the Σ^0 is determined at four center-of-mass angles and found to be small everywhere. Based on published results for the reaction $\pi^+ + p \to \Sigma^+ + K^+$, a comparison of the polarizations of Σ^+, Σ^-, and Σ^0 is made from the charge-independence triangle. A conclusion is reached that the Σ^- polarization should be large, and that the Σ^- and Σ^+ polarizations should be opposite in sign.

I. INTRODUCTION

During the summer and fall of 1960 the 72-inch hydrogen bubble chamber was exposed to both π^+ and π^- beams of 1170 MeV/c momentum. This was done as part of the Associated Production Experiment under the supervision of Professor Frank S. Crawford, Jr. The π^+ film has been analyzed and the results published by Crawford, Grard, and Smith;[1] the results of some of the π^- film are described in this paper. The emphasis here is placed on two things. We wish to examine some of the consequences of charge independence and to determine the polarizations of the hyperons.

It has been known for some time that the cross sections for the reactions

$$\pi^+ + p \to \Sigma^+ + K^+,$$

$$\pi^- + p \to \Sigma^- + K^+,$$

and

$$\pi^- + p \to \Sigma^0 + K^0$$

at incident pion momenta around 1 GeV/c barely satisfy the assumption of charge independence.[2-7] The suggestion has been made that in this region the simplifying assumption of a collinear or "flat" charge-independence triangle is satisfied (see Appendix A).[3,7] That is, the equality holds in the relation:

$$(2\sigma^0)^{1/2} \leqslant (\sigma^+)^{1/2} + (\sigma^-)^{1/2},$$

at least for some production angles. (σ^+ is the cross section for the production of Σ^+ by the above reaction, σ^0 for Σ^0, etc.). We use this equality in Section V to derive some conclusions about hyperon polarizations.

At this momentum we are sufficiently far above threshold to expect the Σ^0 to be polarized. Since the decay of the Σ^0 is a parity-conserving electromagnetic one, the polarization is not easily observed, and in fact there are no published results. The Σ^0 polarization is related to the polarization of the Λ resulting from the $\Sigma^0 \to \gamma + \Lambda$ decay, and this Λ polarization can be observed in the weak Λ decay. We have obtained the Σ^0 polarization by this method.

II. EXPERIMENTAL PROCEDURE

The film for this experiment was exposed in the 72-inch hydrogen bubble chamber at the Bevatron.

Almost all this discussion is based on 34 consecutive rolls of film containing approximately 20,500 pictures. The determination of the Σ^0 polarization uses events taken from a much larger sample of 153 rolls of film, which is not completely analyzed at present.

A. The Beam

The π^- beam-transport system was designed and built by Professor Frank S. Crawford, Jr.[8] Since it has been previously described,[*] we give only a brief survey. A schematic diagram of the beam optics is given in Fig. 1. The single most important characteristic of the beam is a very good momentum resolution. The calculated momentum distribution is shown in Fig. 2, where we see a calculated full width of 6.2 MeV/c. The distribution was also determined from the fitted beam momentum of measured double-vee events. From this we find a full width of 10.4 MeV/c; this larger value is probably due to magnet drift and careless settings over the period of running. Nevertheless, the fractional momentum bite $\Delta P/P$ is still only $\pm 0.5\%$. The relatively monochromatic incident-pion flux is very desirable for such problems as the discrimination between Σ^0 and Λ productions, and generally makes the experiment much cleaner. The bubble chamber magnetic field was kept at its maximum value of 17.9 kG throughout the run. There were on the average 17.4 tracks per picture entering parallel to within ± 0.5 degree.

---

[*]The beam discussed in Reviews of Modern Physics has a nominal momentum of 1030 MeV/c. This film was taken with the magnet currents scaled up to provide 1170 MeV/c.
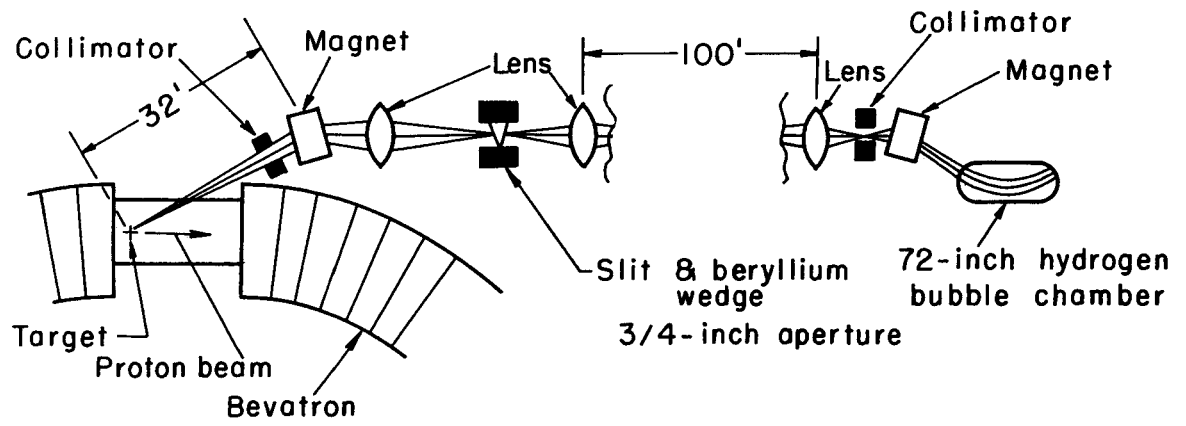
Fig. 1. Schematic diagram of beam optics.
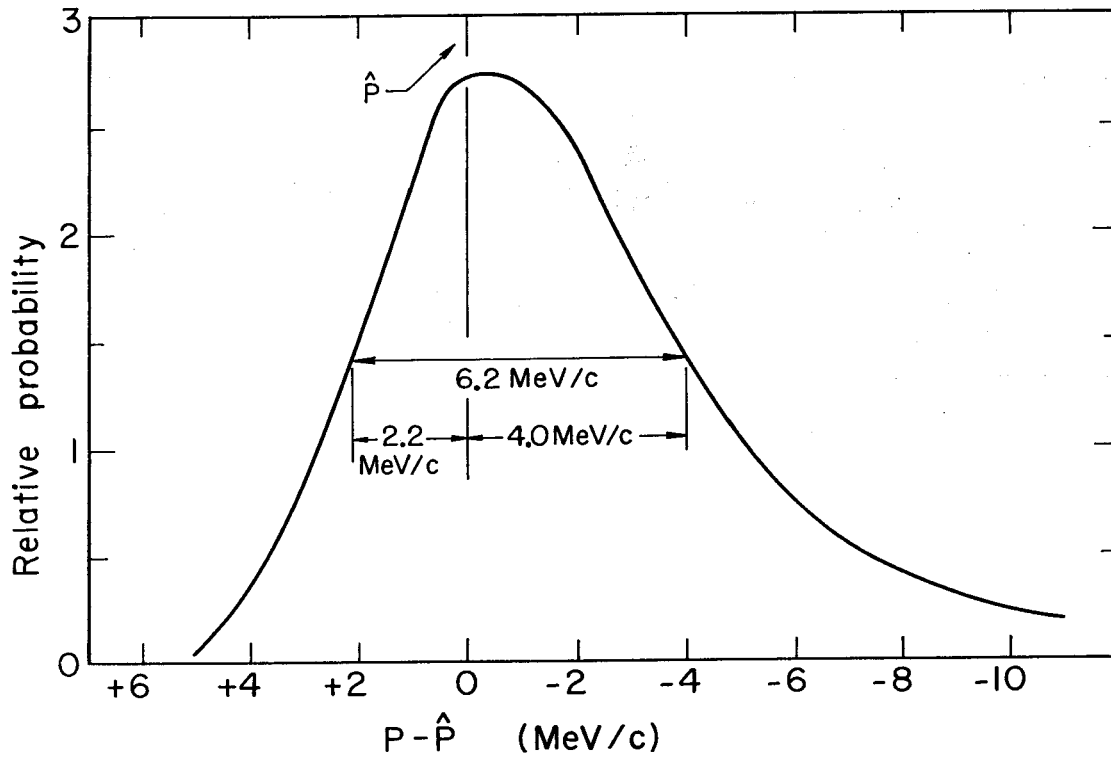
Fig. 2. Momentum distribution of the pion beam at
the center of the chamber, calculated from the
geometry and from the Landau straggling in the
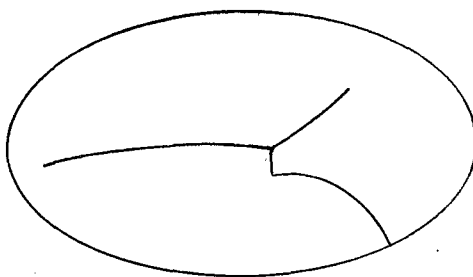chamber windows and hydrogen.

B. Scanning

The film was scanned only for strange-particle production.[9] At this momentum the possible reactions are

$$\pi^- + p \rightarrow \Lambda + K^0 , \tag{1}$$

$$\pi^- + p \rightarrow \Sigma^0 + K^0, \tag{2}$$

$$\pi^- + p \rightarrow \Sigma^- + K^+ . \tag{3}$$

Extra π^0 production is so small as to be negligible. The first two reactions manifest themselves as single- or double-vee topologies.

or
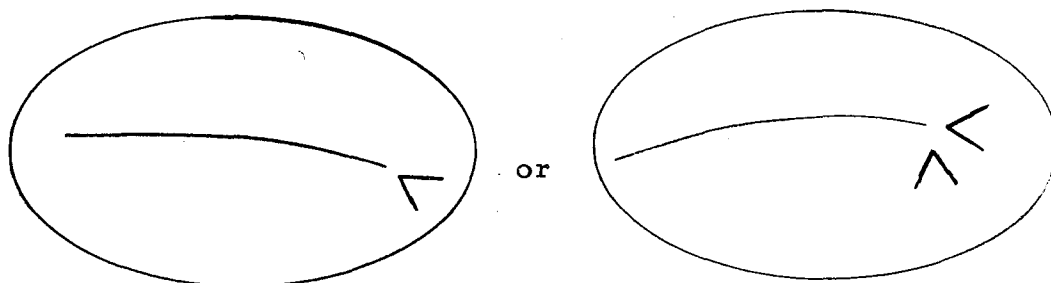
The third reaction also has a very characteristic look.

All three reactions are easily distinguishable from the background of nonstrange events, and the scanners were instructed to record only these interesting events.

Events were rejected by the scanners for the following reasons:

a. Incident track is non-beam, i.e., obviously differing in angle and momenta from the other beam tracks.

b. Incident track has had previous interaction.

c. Too many tracks in the frame for accurate scanning (usually 30 or more).

d. Length of a neutral track is less than 3 mm on the scanning table. (This prevented us from measuring large numbers of two-prong events. The scanning table cutoff corresponds to about 4.5 mm in space, and our final acceptance criterion was 8 mm in space. These rejections were taken into account in the calculation of the absolute cross sections.)

The film was 100% second-scanned. The scanning efficiency of the first scan was found to be 95%, and the cross sections were adjusted accordingly. Events found only in the second scan were not included in the sample.

Fifteen of the thirty-four rolls of film were scanned in five frames each for a beam-track count. This was necessary to determine the incident flux for the cross-section calculations. In the 75 frames, 1306 beam tracks were counted, which satisfied the acceptance criteria of nominal momentum and entrance angle.

After correcting for a 6.25% muon-electron contamination we have 16.3 pion tracks per frame.[10] A frame count showed 18,309 frames scanned, and our average track length was 145 cm. These numbers result in a total path length of 43.33×10^{6} centimeters.

III. DATA PROCESSING

The data were handled in the fashion that has become almost universal in bubble chamber experiments. The events were measured on the "Franckenstein" measuring projector and processed through the standard Alvarez Group PANAL-PACKAGE-EPC programs.[11] The PANAL-PACKAGE-EPC system performs the spatial reconstruction and the kinematic fitting. Fits were attempted for Λ-K and Σ-K decays and production for the vee-type events, and Σ^--K^+ for the charged events. No extra π^0 production was considered. The only events that could not be completely constrained were those single-vee Λ decays which originally came from Σ^0 production.
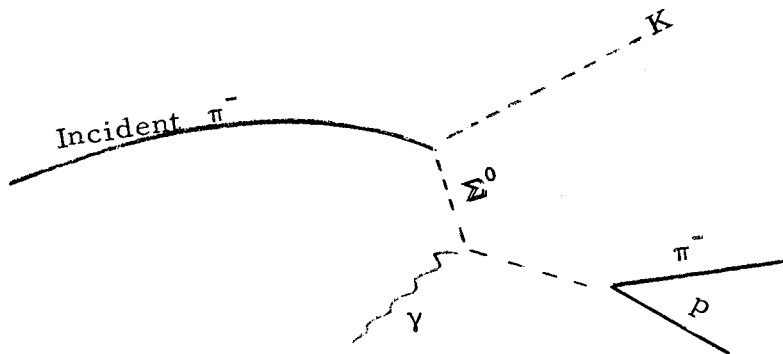
Although the decay vertex could be identified, the production vertex could not be fitted. The treatment of these events is discussed later under "Special Handling."

Unusual events such as rare decay modes, extra π^0 production, hyperon interactions, etc. were verified by using the Alvarez Group QUEST system.[12] QUEST is an on-line event-type program whereby the physicist can test various hypotheses through a typewriter connected to the IBM 709 computer. The computer returns the χ^2 value for the hypothesis and allows kinematic variables to be saved for use at future vertices. The QUEST system was also extremely useful in "cleaning up" the difficult failing events.

A. EXAMIN and Library Programs

The general morphology of the data-processing system is shown in Fig. 3. In this system the program APE EXAMIN forms the heart of the analysis scheme.[13] It is APE EXAMIN that looks at the results of the kinematic fitting and decides on the physical interpretation by use of a χ^2 cutoff. This cutoff was set at a probability level of 0.3% for each constraint class.

Constraint Class	0.3% probable χ^2 level
1	8.6
2	11.6
3	14.0
4	16.0

The APE EXAMIN interpretation of the event was found to agree with a physicist's interpretation virtually 100% of the time. This is largely because the kinematics are such that ambiguous interpretations are quite rare.

It is to be stressed just how important this "in core" interpretation is, since the physicist is now in a position to calculate only the interesting quantities pertaining to a particular physical interpretation. For example, suppose a double-vee event was a Σ^0-K^0 production with the left-hand vee being the K, the calculation then proceeds quite differently than if the double-vee event was a Λ-K production, or even if it were a Σ-K production with the right-hand vee being the K. All the interesting quantities for a event were then written on a data-summary tape (DST). This tape is input to the two subsequent library programs ORDER and LIST AND COMPARE, which compare each event against the scan list, and write all the good passing events out on a DST* tape. All histograms and physics calculations are done on this tape, either with the Alvarez Group summary-examining program SUMX or with programs especially written for each purpose.

The library programs furnish a list of rejected events. These were remeasured after a careful examination on the scanning table. Events were separated out if they were considered unmeasurable. This happened primarily because of tracks' being too short to measure or crossing tracks' obscuring the vertex. Approximately 1% of the events were unmeasurable.
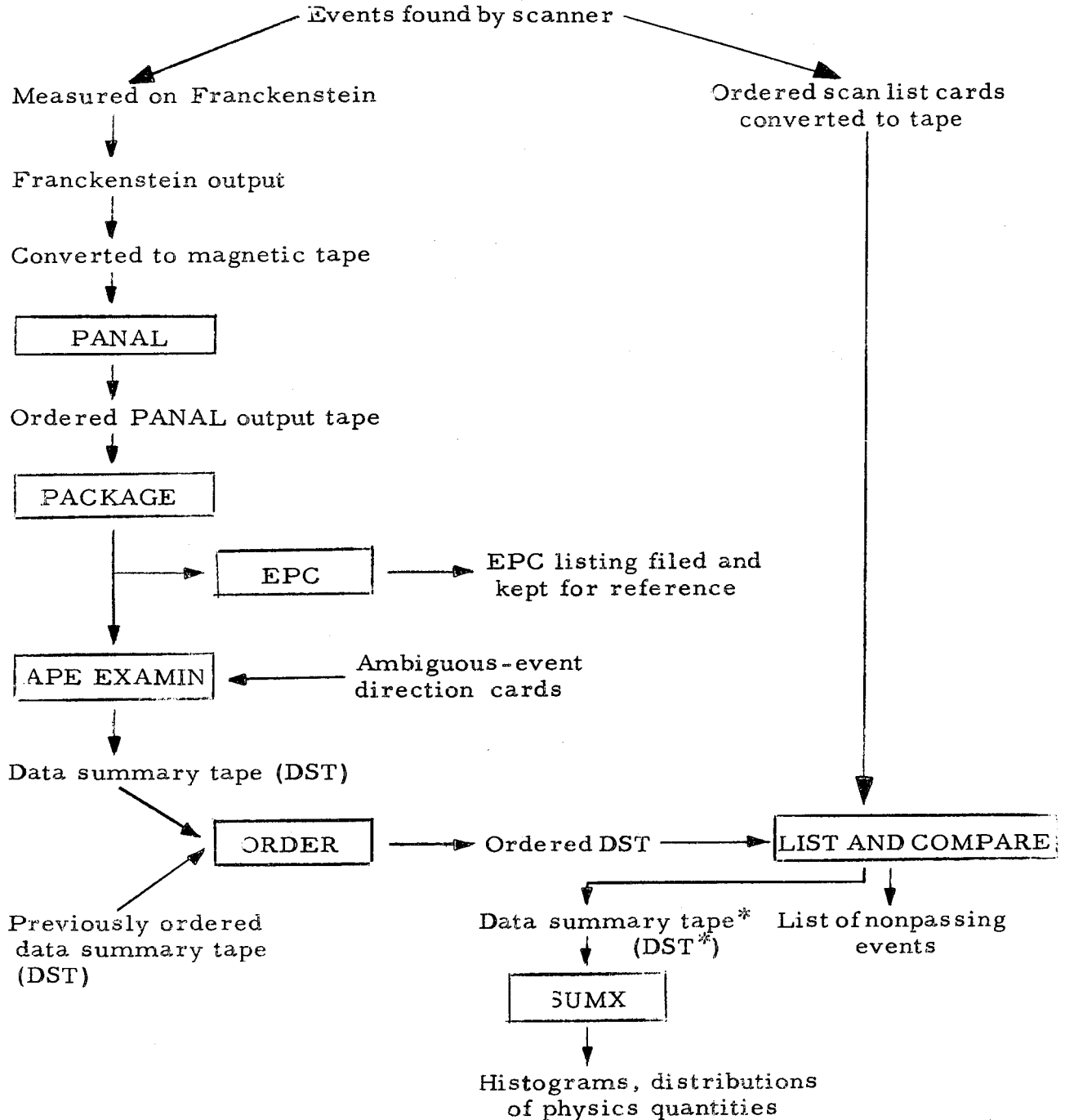
DATA ANALYSIS SYSTEM

Fig. 3. Diagram of the data-processing system. Rectangular blocks correspond to IBM 7090 computer programs.

B. Special Handling

There are two types of events that require special handling. The first type is events that have been given ambiguous interpretations by the APE EXAMIN program. These are almost always single-vee events. If an event has received an ambiguous interpretation on several measurements, the event is decided on the basis of ionization. Fortunately this can always be easily done, since in the region of ambiguity between Λ and K decay at this momentum, the proton track from the Λ decay is quite heavily ionizing.

After an interpretation has been made by the physicist, the APE EXAMIN program is given a card directing it to give the event the desired interpretation, and to perform the calculations for that interpretation. After this stage the event is treated in the ordinary manner. The entire procedure described here was actually used very little in this particular experiment, since less than 1% of the events were ambiguous.

The second kind of event to receive special treatment is the single-vee event, where the decay vertex fits Λ decay, but there is no passing fit for the production. The production vertex of an event which is Σ^0-K production followed by only a Λ decay cannot be fitted by PACKAGE. These events fall into this semifailing type and the APE EXAMIN program assigns them a special interpretation.

If an event received this special interpretation twice it was considered a Σ^0 candidate. The following things were done:

1. By use of the fitted Λ momentum and the measured incident momentum, the missing mass squared recoiling against the Λ was calculated for each candidate.

2. The allowed missing-mass spectrum was calculated. The curve in Fig. 4 shows this spectrum. It extends from 0.286 GeV^2 to 0.388 GeV^2 for incident momentum 1170 MeV/c. The mass squared of the K^0 meson is 0.248 GeV^2. Thus the reactions

$$\pi^- + p \rightarrow \Lambda + K^0$$
$$\pi^- + p \rightarrow \Sigma^0 + K^0$$
$$\quad \rightarrow \gamma + \Lambda$$
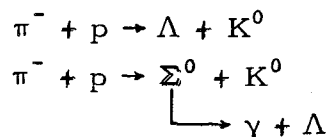
are separated by 0.038 GeV^2 in missing mass squared recoiling against the Λ.
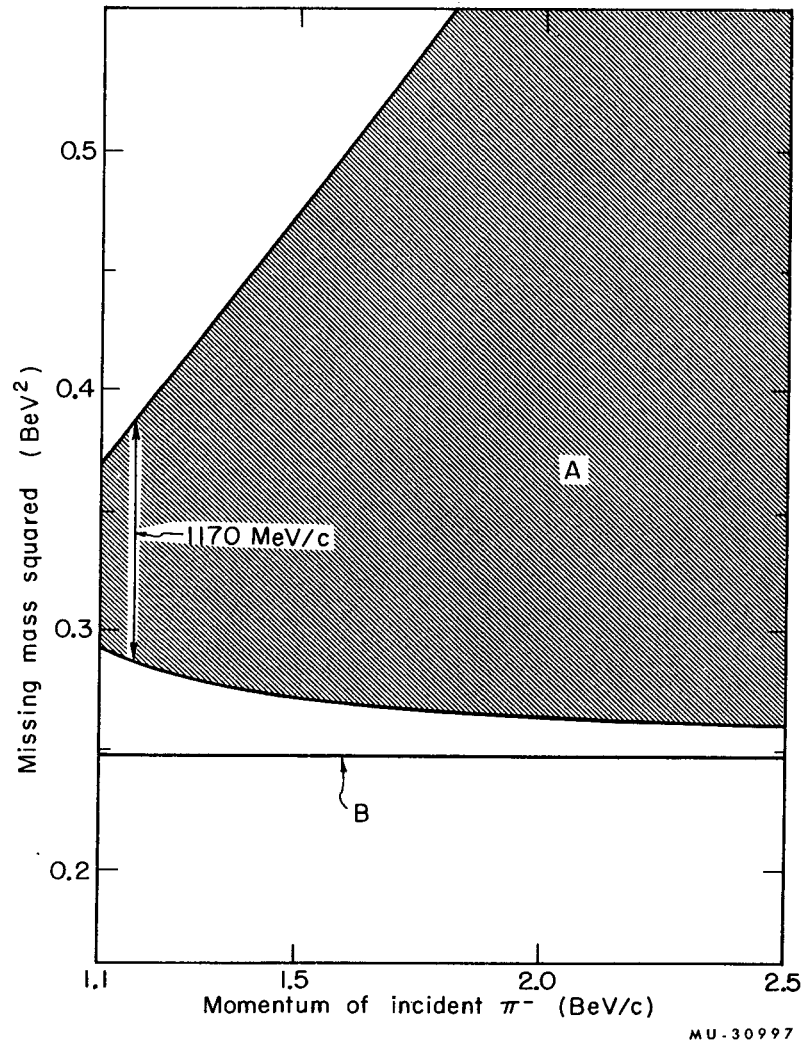
Fig. 4. Allowed region for the square of the missing mass recoiling against the Λ for the reactions

$$\pi^- + p \to \Sigma^0 + K^0$$
$$\quad\quad\quad \hookrightarrow \gamma + \Lambda \quad\quad\quad (A)$$
$$\pi^- + p \to \Lambda + K^0 \quad . \quad\quad (B)$$
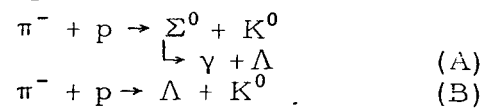
In Reaction B, the square of the missing mass is just the kaon mass.

3. A histogram, Fig. 5, was made of the missing mass for the direct Λ-K events with good fits. Because of measuring errors the spectrum extends to 0.30 GeV^2. A second histogram was made for the Σ-K events with good fits on the same graph, using the double-vee events. This spectrum extended down to 0.275 GeV^2. The region of overlap is 0.275 to 0.300 GeV^2.

4. All Σ^0-K^0 candidates with missing mass squared between 0.300 and 0.400 GeV^2 were accepted as actual Σ-K events. Candidates with missing mass squared in the region of overlap were carefully checked for other possible causes of production failure and remeasured. If there was no difficulty with the event, the production consistently failed, and the missing mass squared was consistently in the overlap region, the event was accepted as a Σ-K production.
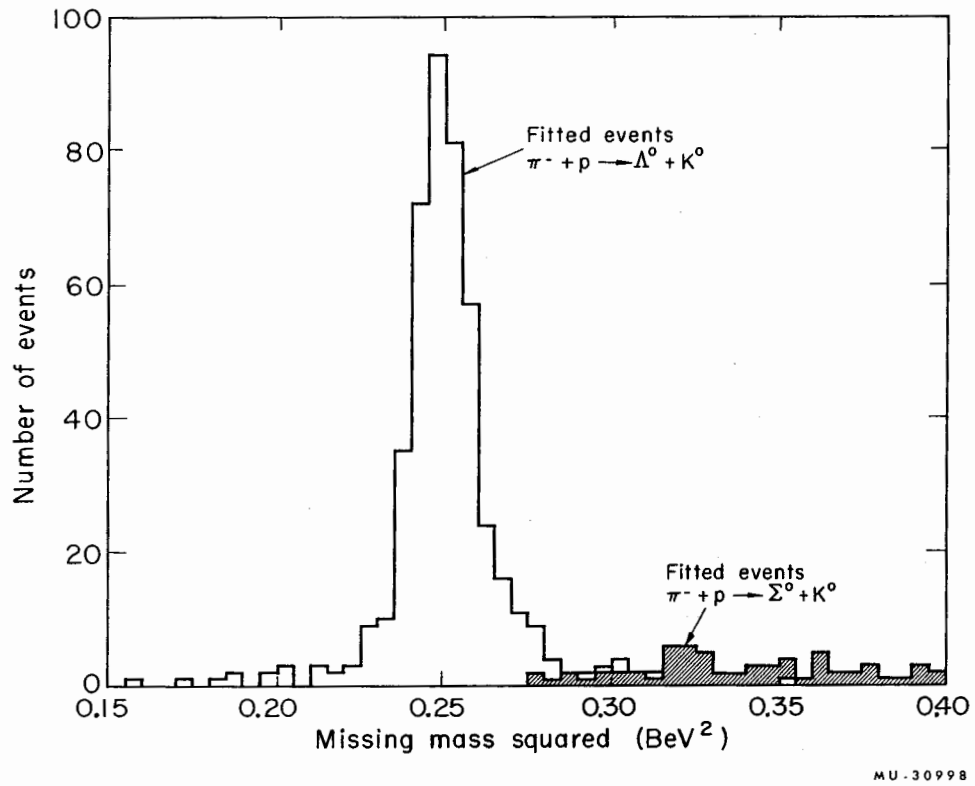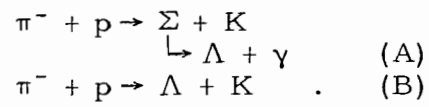
Fig. 5. Experimental spectrum of the missing mass squared recoiling against the Λ in the reactions

$$\pi^- + p \to \Sigma + K$$
$$\hookrightarrow \Lambda + \gamma \quad \text{(A)}$$
$$\pi^- + p \to \Lambda + K \quad . \quad \text{(B)}$$

III. ANALYSIS AND RESULTS

A. Corrections to the Data

There are basically two philosophies toward applying corrections to the data. One can either apply corrections to the final histograms, or alternatively, one can calculate a correction factor for each event and construct histograms of these corrected events. This latter procedure was followed here.

The following corrections were made:

1. Beam attenuation. The attenuation of the π^- beam through the hydrogen in the chamber was accounted for by the factor

$$\epsilon_1 = \exp\left[-(y-y_0)/\bar{x}\right],$$

where y is the position of the event in the chamber measured along the beam, y_0 is the entrance position of the beam, and $\bar{x}$ is the mean free path of π^- in hydrogen at 1170 MeV/c. We assumed a total interaction cross section of 37 mb, corresponding to $\bar{x} = 772$ cm.

2. Fiducial volume. Events were accepted only if they were produced inside a clearly visible region of the chamber. The vee events were also required to decay at least 8 mm from the production point. Thus we accepted events that decayed between $l_1 = 8$ mm and $l_2 =$ the line-of-flight distance to the wall. The accepted events were weighted by a correction factor.

For lambdas the factor is

$$\epsilon_2^\Lambda = \exp\left[-l_1/\gamma\beta c\tau_\Lambda\right] - \exp\left[-l_2/\gamma\beta c\tau_\Lambda\right],$$

where $\gamma\beta$ is calculated for the particle in the laboratory system, c is the speed of light, and τ_Λ is the Λ lifetime. The correction factor is the same for K's except τ_K replaces τ_Λ.

For the Σ^- events no outside fiducial correction was applied, since all events decayed in a short distance. The l_1 is set at 3 mm for the Σ^- events, giving

$$\epsilon_2^\Sigma = \exp\left[-l_1/\gamma\beta c\tau_\Sigma\right].$$

B. Cross Sections

The total path length in this experiment was 43.33×10^6 cm. This corresponds to 0.66 μb/event. The total cross sections are given in Table I. The relationship between these cross sections and other known points is given in Figs. 6 and 7.

The differential cross section for $\pi^- + p \rightarrow \Lambda + K$ is given in Fig. 8. The smooth curve is a least-squares fit to $\cos^3\theta$. It has a 37% probability of being a good fit. The $\cos^3\theta$ dependence required by Wolf et al.[8] at 1030 MeV/c is still present at 1170 MeV/c, although not as pronounced. The coefficients of the fitted curves are given in Tables II and III.

The product of cross section times polarization for the Λ events is shown in Fig. 9. It is fitted to $\sin\theta \cos^2\theta$ with a probability of 47%. Table I shows that the average polarization is consistent with 100%, if we assume Cronin and Overseth's value[19] of $a_\Lambda = -0.62 \pm 0.05$.

The Σ^- differential cross section and polarization are shown in Figs. 10 and 11. The average polarization given in Table I is 1.5 standard deviations from zero, but no significance is attached to this.

The Σ^0 differential cross section is given in Fig. 12. This is used in calculating the charge-independence triangle. The Σ^0 polarization is discussed in a subsequent section.

C. The Σ Triangle

By using the results of Crawford, Grard, and Smith[1] for the cross section of $\pi^+ + p \rightarrow \Sigma^+ + K^+$ and our results for $\pi^- + p \rightarrow \Sigma^- + K^+$ and $\pi^- + p \rightarrow \Sigma^0 + K^0$, we can construct the charge-independence triangle. Figure 13 shows the data for $(\sqrt{\sigma_+} + \sqrt{\sigma_-})$ and $\sqrt{2\sigma_0}$. These are all plotted vs the cosine of the center-of-mass angle of the Σ. Charge independence requires the charged amplitudes (▲) to lie above the neutral amplitude (●). (See Appendix A.) This is slightly violated in the backward hemisphere; however, it is not statistically significant. The two sets of data lie quite close to each other in this region, and we make the assumption that they are nearly equal for $\cos\theta < 0$. This allows us to draw some conclusions about the Σ^- polarizations in Section IV.

Table I. Cross sections and polarizations at an incident
π^- momentum of 1170 MeV/c

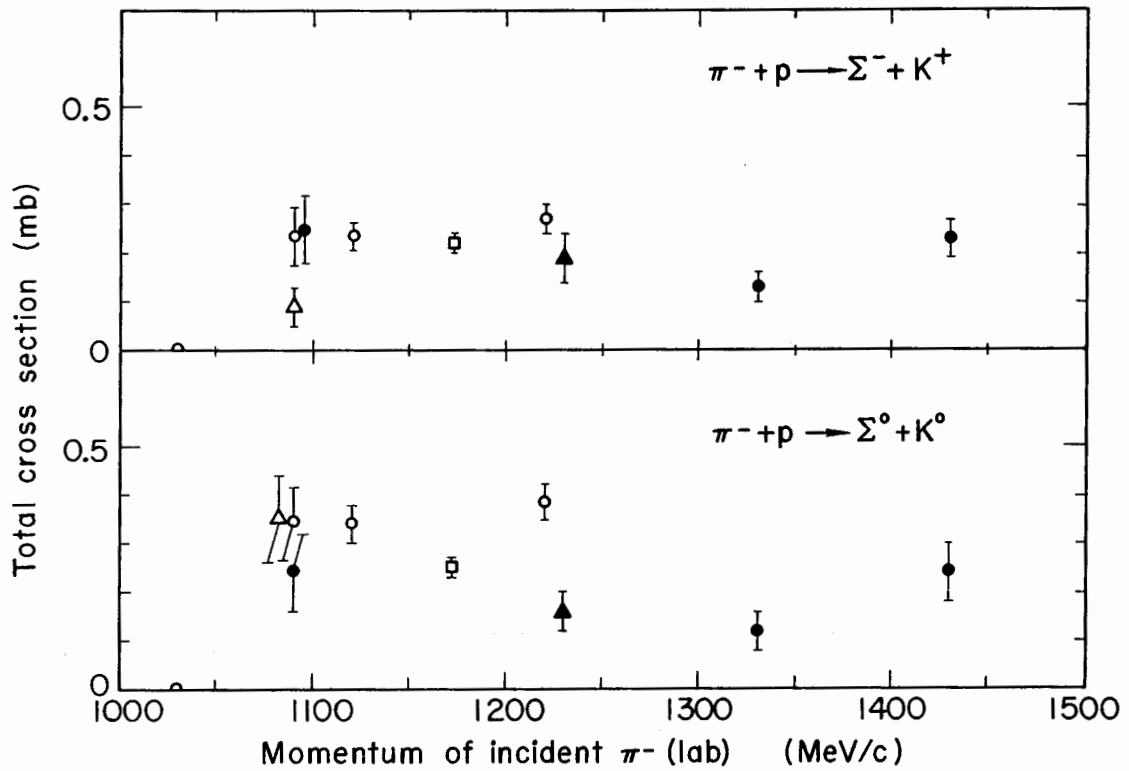| Reaction	Cross section (μb)	Number or events
$\pi^- + p \rightarrow \Lambda + K^0$	528±29	379
$\pi^- + p \rightarrow \Sigma^0 + K^0$	248±18	198
$\pi^- + p \rightarrow \Sigma^- + K^+$	210±13	276

Polarizations

$$a_\Lambda \langle P_\Lambda \rangle = 0.67 \pm 0.10$$

$$a^- \langle P_{\Sigma^-} \rangle = -0.15 \pm 0.10$$

$$a_\Lambda \langle P_{\Sigma^0} \rangle = 0.08 \pm 0.16$$
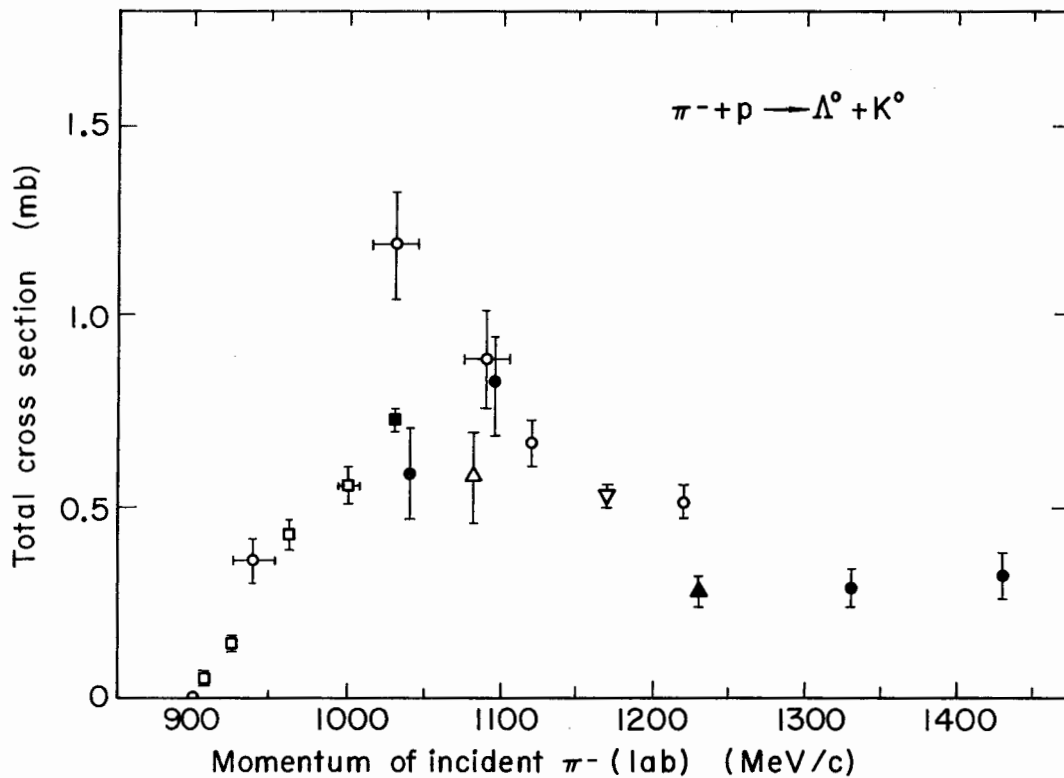
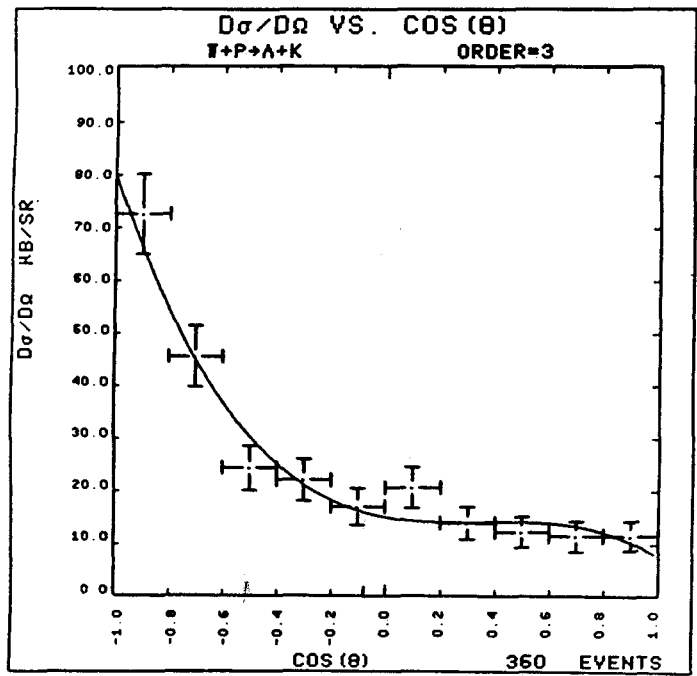Fig. 6. Total cross section for the reaction
$\pi^- + p \rightarrow \Lambda + K^0$.

O Ref. 14	▲ Ref. 2
● Ref. 15	□ Ref. 17
△ Ref. 16	■ Ref. 18
▽ This experiment	

MU-30999

Fig. 7. Total cross sections for $\pi^- + p \rightarrow \Sigma^- + K^+$
and $\pi^- + p \rightarrow \Sigma^0 + K^0$.

      O Ref. 14   ▲ Ref. 2

      ● Ref. 15   □ This experiment

      △ Ref. 16

Fig. 8. Differential cross section for $\pi^- + p \to \Lambda + K^0$. The smooth curve is a least-squares fit up to and including $\cos^3\theta$.

Table II. Coefficients determined from a least-squares
fit of the cross sections to the expansion

$$\sigma(\theta) = \sum_{L=0} A_L \cos^L \theta$$

Reaction	Coefficients A_L	Probability of fitting (%)
$\pi^- + p \rightarrow \Lambda + K^0$ (Fig. 8)	$A_0 = 26.0 \pm 3.0 \mu b/sr$ $A_1 = -15.7 \pm 8.6 \mu b/sr$ $A_2 = 47.5 \pm 8.5 \mu b/sr$ $A_3 = -44.3 \pm 15.0 \mu b/sr$	37
$\pi^- + p \rightarrow \Sigma^- + K^+$ (Fig. 10)	$A_0 = 10.0 \pm 1.2 \mu b/sr$ $A_1 = 5.4 \pm 1.8 \mu b/sr$ $A_2 = 15.0 \pm 3.3 \mu b/sr$	85
$\pi^- + p \rightarrow \Sigma^0 + K^0$ (Fig. 14)*	$A_0 = 28.9 \pm 3.3 \text{ counts}/sr$ $A_1 = 8.6 \pm 5.0 \text{ counts}/sr$ $A_2 = 46.9 \pm 9.6 \text{ counts}/sr$	58

*This angular distribution is not normalized to an absolute cross section.

Table III. Coefficients determined from a least-squares fit of the product of cross section times polarization to the expansion[*] $\sigma a P = \sum\limits_{L=0} B_L \sin\theta \cos^L\theta$
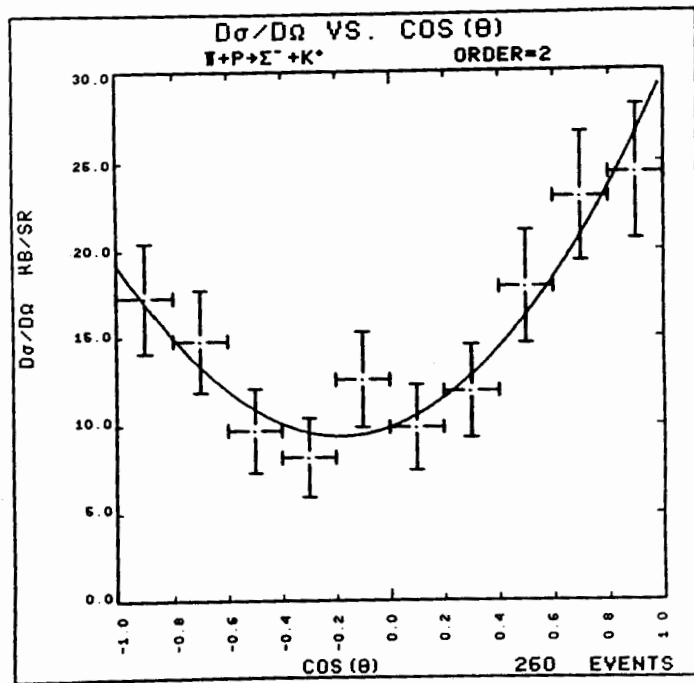
Reaction	Coefficients B_L (μb)	Probability of fitting (%)
$\pi^- + p \to \Lambda + K^0$ (Fig. 9)	$B_0 = 11.2 \pm 3.4$ $B_1 = -18.4 \pm 6.4$ $B_2 = 37.3 \pm 13.4$	48
$\pi^- + p \to \Sigma^- + K^+$ (Fig. 11)	$B_0 = -4.0 \pm 1.7$	94

[*] a is the asymmetry parameter in the hyperon decay.
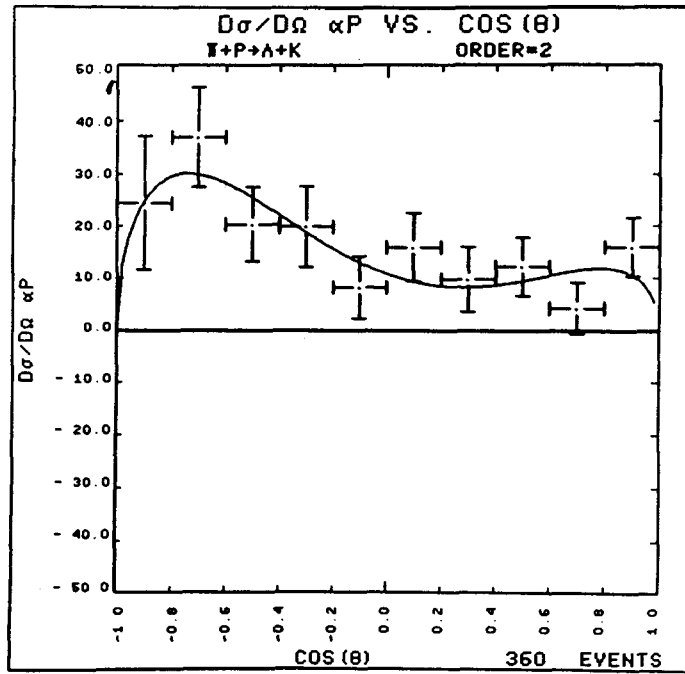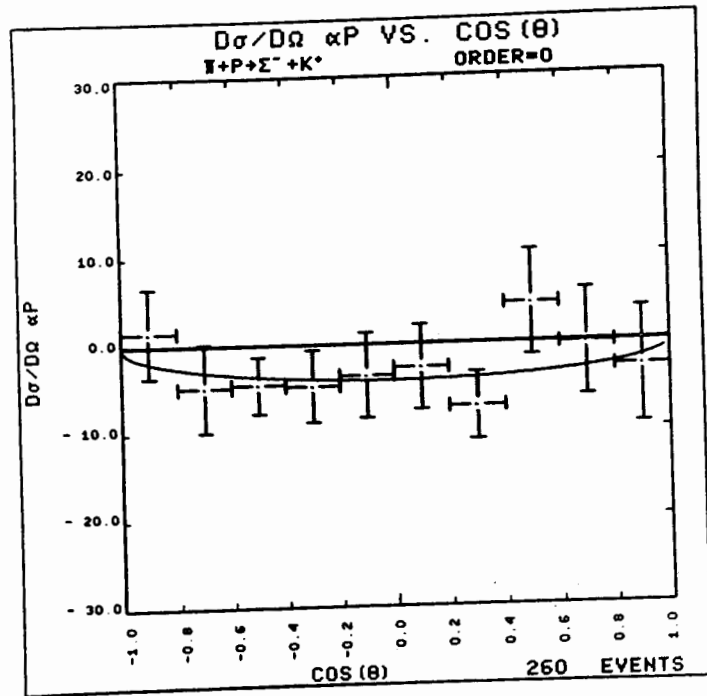
MU-31002

Fig. 9. Cross section times polarization for
$\pi^- + p \to \Lambda + K$. The smooth curve is a
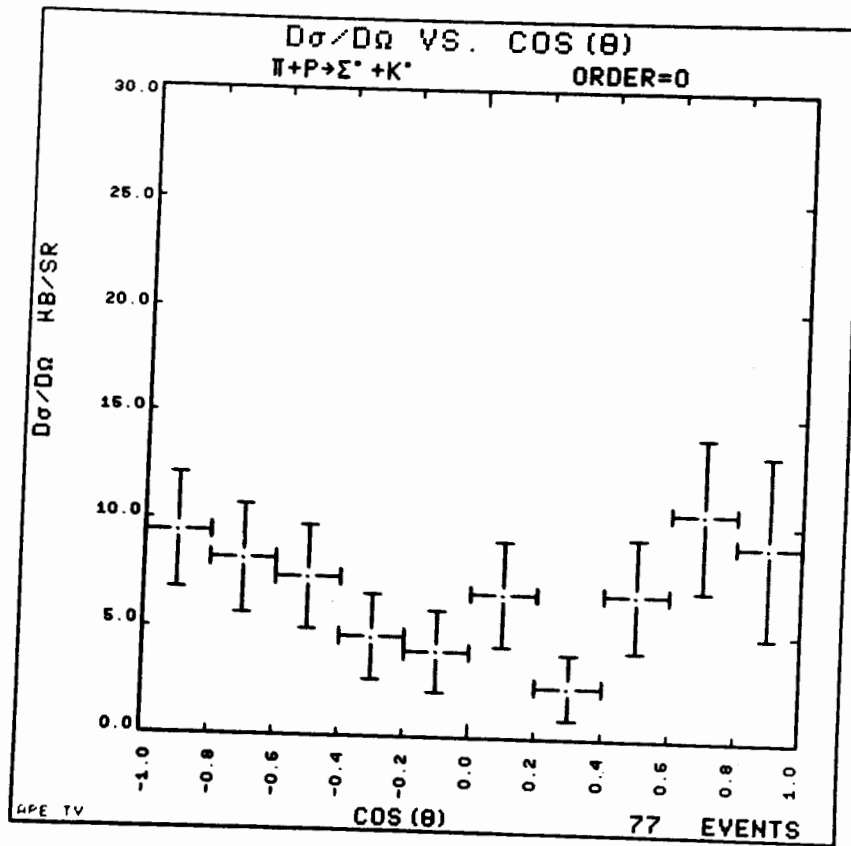least-squares fit up to and including
$\sin\theta \cos^2\theta$.

Fig. 10. Differential cross section for $\pi^- + p \to \Sigma^- + K^+$ fitted up to and including $\cos^2\theta$.

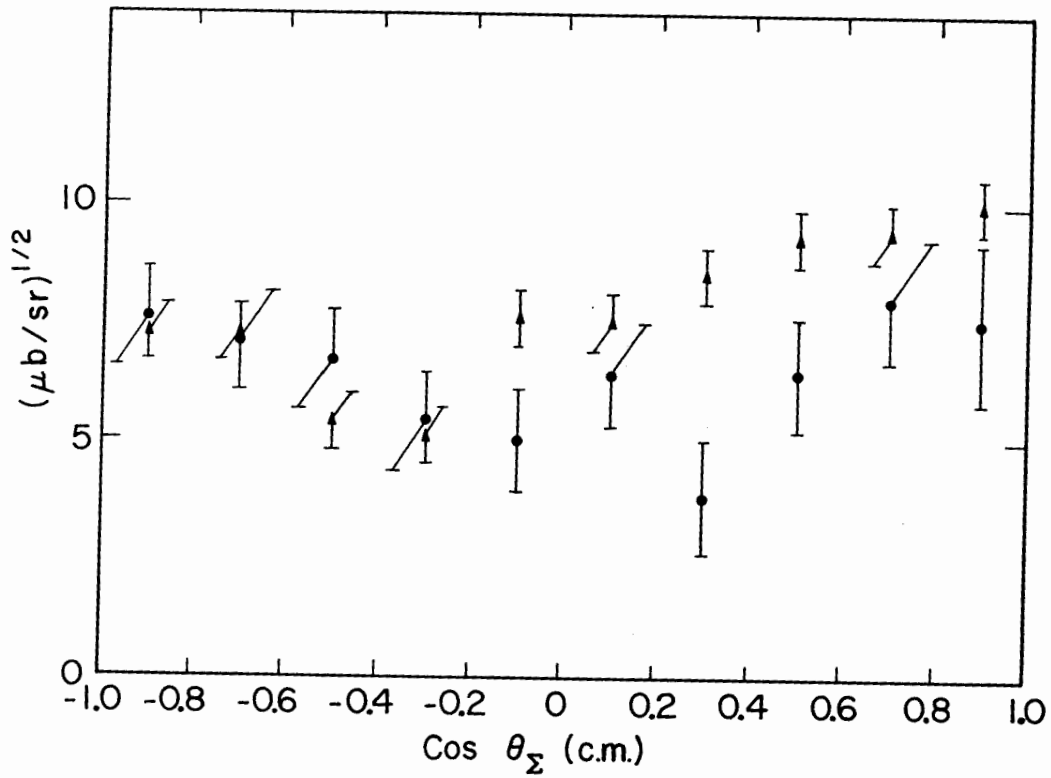Fig. 11. Cross section times polarization for
$\pi^- + p \rightarrow \Sigma^- + K^+$ fitted to $\sin\theta$.

Fig. 12. Differential cross section for the reaction
$\pi^- + p \rightarrow \Sigma^0 + K^0$.

Fig. 13. Charge independence triangle for the three reactions $\pi^- + p \rightarrow \Sigma^- + K^+$, $\pi^- + p \rightarrow \Sigma^0 + K^0$, and $\pi^+ + p \rightarrow \Sigma^+ + K^+$, all at 1170 MeV/c incident pion momentum.

▲: Σ^+ amplitude + Σ^- amplitude
●: $\sqrt{2} \times \Sigma^0$ amplitude.

MU-31005

D. The Σ^0 Polarization

Since the sample of Σ^0 events available in the 34 rolls of film was too small to permit us to make any statements about the polarization, events were included from another much larger sample. This was film at the same momentum but incompletely analyzed at present and as such, not avilable for cross-section measurements. The events were handled in exactly the same way as already described.

The final sample was 322 double-vee-type Σ^0 events. The angular distribution of these events is shown in Fig. 14. It is fitted by a power series up to $\cos^2\theta$ with a probability of 57%.

The electromagnetic decay of the Σ^0 can be completely analyzed theoretically, with the result[20] that the polarization of the Λ resulting from Σ^0 decays is related to the polarization of the Σ^0's by

$$\underset{\sim}{P}_\Lambda = - (\underset{\sim}{P}_\Sigma \cdot \hat{q})\hat{q}$$

where $\hat{q}$ is the direction of the line of flight of the Λ in the Σ^0 center-of-mass system.

Now we do the following things:

(a) Assume the Σ is polarized along the normal to the production plane $\hat{n}$.

(b) Let $\hat{k}$ be the direction of the π^- from the Λ decay in the Λ center-of-mass system.

(c) Assume the well-known form of the distribution of pions in the Λ decay,

$$\frac{\partial N}{\partial (\underset{\sim}{P}_\Lambda \cdot \hat{k})} = \frac{N}{2} (1 + a_\Lambda \underset{\sim}{P}_\Lambda \cdot \hat{k}) ,$$

where N is the number of events, P is the Λ polarization, and a_Λ is the Λ-decay asymmetry parameter.

So if the π^- from polarized Λ's are distributed according to the above relation, and we use only Λ's coming from Σ^0's, the π^- distribution is
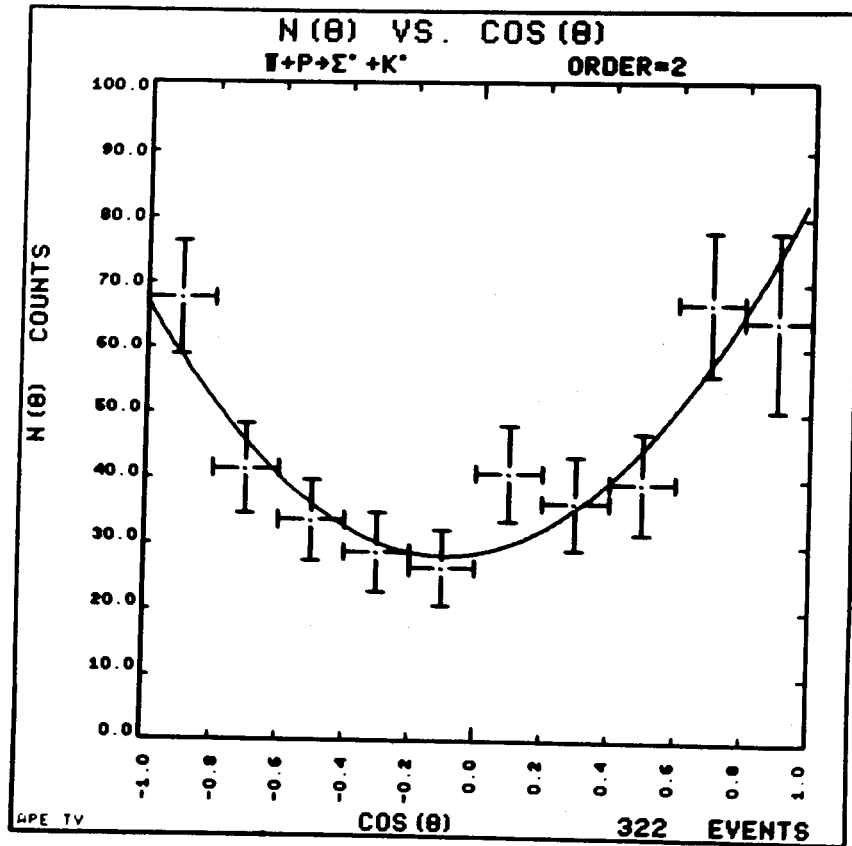
Fig. 14. Angular distribution for the reactions $\pi^- + p \rightarrow \Sigma^0 + K^0$ fitted up to and including $\cos^2\theta$.

$$\frac{\partial^2 N}{\partial \xi \partial \eta} = \frac{N}{4} \left[1 - (a_\Lambda P_\Sigma) \xi \eta \right] ,$$

where ξ and η are $(\hat{n} \cdot \hat{q})$ and $(\hat{k} \cdot \hat{q})$, respectively, and $P_{\Sigma^0} = |P_{\Sigma^0}|$.

Using this distribution, we measure the polarization of the Σ^0's at four angles of production, Fig. 15. Our result for the average value is $a_\Lambda \langle P_{\Sigma^0} \rangle = 0.08 \pm 0.16$ and if we use[19] $a_\Lambda = -0.62 \pm 0.05$ we get $\langle P_{\Sigma^0} \rangle = -0.13 \pm 0.26$. By confining ourselves to the backward hemisphere, $\cos \theta \leqslant 0$, we have $\langle P_{\Sigma^0} \rangle = 0.06 \pm 0.39$. We conclude that the Σ^0 polarization is small and consistent with zero within our rather large errors.
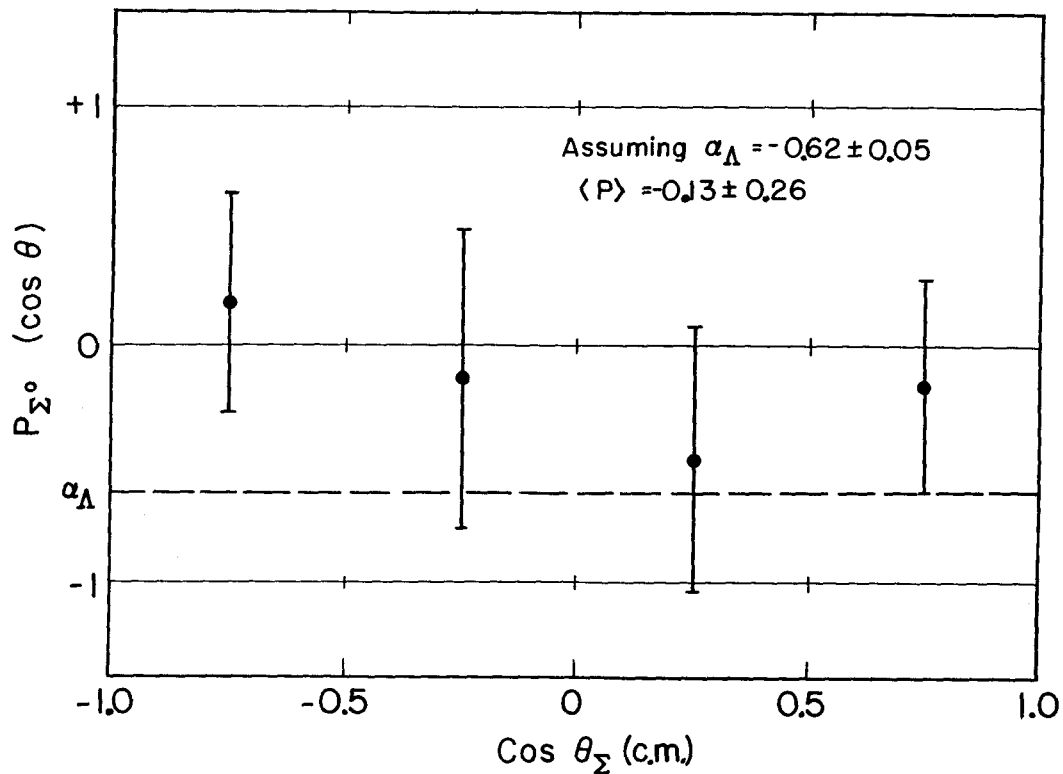
Fig. 15. Polarization of Σ^0 in the reaction
$\pi^- + p \rightarrow \Sigma^0 + K^0$ at 1170 MeV/c.

V. DISCUSSION

Michel has shown[6] that whenever the equality holds in the charge-independence triangle--i. e., the triangle is "flat" or collinear-- then the polarizations of the Σ^-, Σ^0, and Σ^+ are all equal:

$$P_{\Sigma^+} = P_{\Sigma^-} = P_{\Sigma^0} .$$

Unfortunately, this is a very difficult relation to use experimentally, because it is hard to say when the triangle is absolutely flat. If the Michel theorem were true in a fairly large region away from the collinear case, we could assume that the polarizations were equal--say, whenever the two curves of Fig. 13 were equal within their statistical errors. However, Crawford has shown that in fact the polarizations become nonequal very quickly as one moves away from the flat case.[21] In an effort to take this into account Crawford included the first-order corrections to the polarizations as the triangle moved into the nonflat region. He found that although the Michel result is not maintained, the equation

$$P_{\Sigma^+} + P_{\Sigma^-} = 2\, P_{\Sigma^0}$$

does hold in the neighborhood of the flat solution. At the exact flat solution, of course, both the Michel equality and the Crawford solution hold and are consistent with each other.

We can apply the Crawford result to our data in the backward hemisphere ($\cos \theta_\Sigma \leqslant 0$), since there the triangle seems nearly flat within statistics (see Fig. 13). Also, we can use our own independent measurement of the Σ^0 polarization. This requires

$$P_{\Sigma^+} \approx - P_{\Sigma^-} ,$$

since we have determined that $P_{\Sigma^0} \approx 0$ everywhere. The polarization of the Σ^+ has been measured as 80±25% by Crawford, Grard, and Smith. Thus we would suggest that at this momentum the Σ^- polarization is also large and of the opposite sign.

ACKNOWLEDGMENTS

APPENDIX: THE TRIANGLE INEQUALITY

Let A^+, A^-, A^0 be the complex amplitudes for the three reactions

$$\pi^+ + p \to \Sigma^+ + K^+ \, ,$$

$$\pi^- + p \to \Sigma^- + K^+ \, ,$$

$$\pi^- + p \to \Sigma^0 + K^0 \, .$$

The hypothesis of charge independence restricts the three reactions to depend upon only two isotopic spin amplitudes, $A^{1/2}$ and $A^{3/2}$. Using Clebsch-Gordan coefficients to relate the charge states to the isotopic spin states, we have
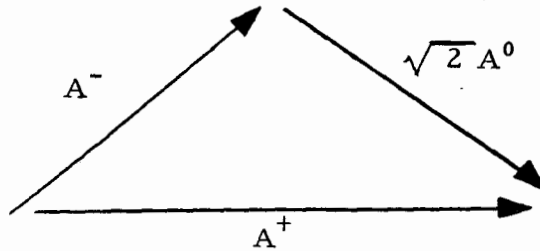
$$A^+ = A^{3/2} \, ,$$

$$A^- = 1/3 \, A^{3/2} + 2/3 \, A^{1/2} \, ,$$

$$A^0 = \sqrt{2/3} \, (A^{3/2} - A^{1/2}) \, .$$

These three equations require

$$A^+ = A^- + \sqrt{2} \, A^0 \, ,$$

which can be visualized as a geometrical relationship between vectors:

As a result the magnitudes of the amplitudes must obey the triangular inequalities—that is, the length of one side compared with the sum of the remaining two. Specifically,

$$|A^+| + |A^-| \geq \sqrt{2} \cdot |A^0|$$

or

$$\sqrt{\frac{\partial \sigma^-}{\partial \Omega}} + \sqrt{\frac{\partial \sigma^+}{\partial \Omega}} \geq \sqrt{2 \frac{\partial \sigma^0}{\partial \Omega}} \quad .$$

This inequality depends only upon the assumption of charge
independence, and is thus a direct test of the hypothesis.

REFERENCES

1. F. S. Crawford, Jr. , Fernand Grard, and Gerald A. Smith, Phys. Rev. 128, 368 (1962).

2. J. L. Brown, D. A. Glaser, D. I. Meyer, M. C. Perl, and J. Vander Velde, Phys. Rev. 107, 906 (1957).

3. F. S. Crawford, Jr. , R. L. Douglass, M. L. Good, G. R. Kalbfleisch, M. L. Stevenson, and H. K. Ticho, Phys. Rev. Letters 3, 394 (1959).

4. A. Berthelot, A. Daudin, O. Goussu, F. Grard, M. Jubiol, F. Levy, C. Lewin, A. Rogozinski, J. Laberrique-Frolow, C. Quannes, and L. Vigneron, in Proceedings of the 1960 Annual International Conference on High Energy Physics at Rochester, (Interscience Publishers, Inc. , New York, 1960), p. 406.

5. C. Baltay, H. Courant, W. J. Finchinger, E. C. Fowler, H. L. Kraybill, J. Sandweiss, J. R. Sanford, D. L. Stonehill, and H. D. Taft, Revs. Mod. Phys. 33, 374 (1961).

6. J. R. Albright, T. O. Binford, U. Camerini, W. F. Fry, M. Foster, M. L. Good, R. W. Hartung, R. R. Kofler, V. G. Lind, R. P. Matsen, C. T. Murphy, M. W. Peters, D. D. Reeder, D. Stern, G. Tautfest, and R. B. Willman, in Proceedings of the 1962 International Conference on High Energy Physics at CERN, (CERN, Geneva, 1962), p. 276.

7. L. Michel, Nuovo cimento 22, 203 (1961); L. Michel and H. Rouhaninejad, Phys. Rev. 122, 242 (1961).

8. S. Wolf, N. Schmitz, L. Lloyd, W. Laskar, F. Crawford, Jr. , J. Button, J. Anderson, and G. Alexander, Revs. Mod. Phys. 33, 439 (1961).

9. M. Alston and H. Monteros, Data Analysis for the Associated-Production Experiment, Lawrence Radiation Laboratory Alvarez Group Memo No. 165, May 1, 1961.

10. Private communication from Leroy Price, Lawrence Radiation Laboratory; also D. Duane Carmony, The Pion-Pion Cross Section by the Chew-Low Method (thesis), Lawrence Radiation Laboratory Report UCRL-9886, October 1961.

11. A Discussion of PANAL, PACKAGE, SUMX, and other general Alvarez Group programs together with detailed references is found in A. H. Rosenfeld, Current Performance of the Alvarez Group Data-Processing System, Nucl Instr. Methods, 20 (1963) (to be published).

12. H. Alston, J. E. Braley, and P. White, QUEST - An On-Line Event-Processing Routine, Lawrence Radiation Laboratory Report UCRL-10401, August 8, 1962; also M. H. Alston, J. E. Braley, J. Stedman, M. L. Stevenson, and P. White, QUEST Operating Manual, Lawrence Radiation Laboratory Alvarez Group Memo No. 432, May 30, 1963.

13. D. Johnson, The EXAMIN System, Lawrence Radiation Laboratory Alvarez Group Memo No. 331, September 5, 1961.

14. F. S. Crawford, Jr., M. Cresti, M. L. Good, K. Gottstein, E. M. Lyman, F. T. Solmitz, M. L. Stevenson, and H. K. Ticho, in Proceedings of the 1958 Annual International Conference on High Energy Physics at CERN, (CERN, Geneva, 1958), p. 323.

15. J. Steinberger, in Proceedings of the 1958 Annual International Conference on High Energy Physics at CERN (CERN, Geneva, 1958), p. 147.

16. L. B. Leipuner and R. K. Adair, Phys. Rev. 109, 1358 (1958).

17. L. Bertanza, P. L. Connolly, B. B. Culwick, F. R. Eisler, T. Morris, R. Palmer, A. Prodell, and N. P. Samios, Phys. Rev. Letters 8, 332 (1962).

18. F. S. Crawford, Jr., in Proceedings of the 1962 International Conference on High Energy Physics at CERN (CERN, Geneva, 1962), p. 827.

19. J. W. Cronin and O. E. Overseth, in Proceedings of the 1962 International Conference on High Energy Physics at CERN (CERN, Geneva, 1962), p. 453.

20. N. Byers and H. Burkhardt, Phys. Rev. 121, 281 (1961); G. Snow and J. Sucher, Nuovo cimento 18, 195 (1960); R. H. Dalitz, Strong Interaction Physics and Strange Particles (Oxford University Press, London, 1962), Chapter XII.

21. Frank S. Crawford, Jr., Lawrence Radiation Laboratory, private communication.